

Homoclinic bifurcation in a Hodgkin–Huxley model of thermally sensitive neurons

Ulrike Feudel

Department of Physics, University of Potsdam, Potsdam 14415, Germany

Alexander Neiman,^{a)} Xing Pei, and Winfried Wojtenek

Center for Neurodynamics, University of Missouri at St. Louis, St. Louis, Missouri 63121

Hans Braun and Martin Huber

Institute of Physiology, University of Marburg, Marburg 35037, Germany

Frank Moss

Center for Neurodynamics, University of Missouri at St. Louis, St. Louis, Missouri 63121

(Received 3 June 1999; accepted for publication 30 November 1999)

We study global bifurcations of the chaotic attractor in a modified Hodgkin–Huxley model of thermally sensitive neurons. The control parameter for this model is the temperature. The chaotic behavior is realized over a wide range of temperatures and is visualized using interspike intervals. We observe an abrupt increase of the interspike intervals in a certain temperature region. We identify this as a homoclinic bifurcation of a saddle-focus fixed point which is embedded in the chaotic attractors. The transition is accompanied by intermittency, which obeys a universal scaling law for the average length of trajectory segments exhibiting only short interspike intervals with the distance from the onset of intermittency. We also present experimental results of interspike interval measurements taken from the crayfish caudal photoreceptor, which qualitatively demonstrate the same bifurcation structure. © 2000 American Institute of Physics. [S1054-1500(00)02301-6]

A wide class of sensory neurons demonstrates spontaneous oscillatory activity. Moreover, some thermosensitive neurons, for example, electroreceptors of the catfish, dogfish, the warm and cold receptors of rat and cat and the caudal photoreceptor of the crayfish, display complicated bifurcation sequences of the spike train patterns as the control parameter, e.g., the temperature, changes. Recent experiments also revealed the existence of low-dimensional chaotic behavior of some thermoreceptors. In this paper we study a rather unusual behavior of a bursting neuron, modeled by a modified Hodgkin–Huxley system, manifested in an explosion of interspike intervals at a certain temperature value. We identify this transition with a homoclinic bifurcation of a saddle-focus equilibrium state which is embedded in the chaotic attractor of the system. We also demonstrate qualitatively the same phenomenon in electro-physiological experiments with the caudal photoreceptor of the crayfish.

I. INTRODUCTION

In electrophysiological experiments different types of neuronal impulse patterns can be observed ranging from regular or irregular single-spike activity (tonic firing) to more or less rhythmic grouping of impulses (burst discharges). Such temporal patterns are partly ascribed to synaptic interactions within neuronal networks but can also re-

sult from the nonlinear internal dynamics of individual neurons. Here we examine impulse pattern modulation of a Hodgkin–Huxley-type computer simulation which originally was developed to simulate peripheral cold receptors discharges.¹ These receptors encode environmental temperatures into neuronal impulse trains and thereby exhibit a fascinating array of different types of firing patterns which, without doubt, originate from internal dynamics of single receptors. The existence of neuronal networks can be excluded because cold receptors are free nerve endings in the superficial layers of the skin.²

Because of the small size and sparse distribution of cold receptors, intracellular recordings of the membrane potential or ionic currents are not possible so far. The temporal patterns of the discharges, however, clearly indicate that the impulses are generated by an oscillating membrane process of systematic temperature dependencies. This can most easily be seen at mid-temperatures where rhythmic burst discharges are triggered. However, there is also an essential contribution of noise which becomes of particular functional significance especially towards higher temperatures where oscillations with skipings occur.³ This phenomenon can spread all over the complete encoding range in other thermosensitive neurons, e.g., shark electroreceptors.⁴ Moreover, there are other types of irregular discharges, preferably at lower temperatures, which at least partly seem to result from low-dimensional dynamics.¹

More detailed analysis of the impulse pattern indicates that the oscillations arise from subthreshold mechanisms which are independent of spike generation. For example, when one or more oscillation cycles are without spike gen-

^{a)}Author to whom correspondence should be sent. Electronic mail: neiman@neurodyn.umsl.edu

eration, the oscillations obviously continue with an almost unchanged rhythm and, at a given temperature, the period of the burst discharges is almost unaffected by random variations of the number of spikes per burst.^{3,5} The assumption of subthreshold, spike-independent oscillations is additionally supported by electrophysiological recordings under the variation of extracellular calcium concentrations and applications of calcium channel blockers. These experiments indicate that low-threshold calcium channels contribute to the oscillating process, but mainly seem to exert repolarizing effects, probably via Ca-activated K-channels, with neglectable contribution to depolarization.⁶

Several models for the generation of spike-triggering oscillations exist; most of them focus on specific types of patterns of central neurons (e.g., Refs. 7 and 8), others also consider the transitions between regular and chaotic patterns (e.g., Ref. 9) or even directly refer to cold receptor data (e.g., Ref. 10). The model which will be examined here has been developed on the background of the above described experimental findings, i.e., it considers subthreshold oscillations in addition to spike generation. It uses a Hodgkin–Huxley-type approach which, however, is drastically simplified and reduced. Nevertheless, all relevant physiological parameters mentioned above do still have their explicit counterpart in the equations (see Sec. II).

This model, with addition of noise, exhibits all major characteristics of stationary cold receptor discharges¹ and, with slight modifications, can simulate principal neuromodulatory properties also observed in other types of temperature sensitive receptors and neurons.^{11,12} Moreover, new methods for finding unstable periodic orbits¹³ revealed that low-dimensional dynamics contribute to specific irregularities of the patterns which occur in cold receptors as well as in such different neurons as electroreceptors and hypothalamic neurosecretory cells^{14,15} and which, most remarkably, can also be seen in noisy simulation runs of the model under similar stimulus conditions as in the experiments.

One possible way to study the generic properties of low-dimensional chaotic systems is the analysis of bifurcation sequences of limit sets under the variation of a control parameter. Bifurcations of chaotic attractors are often related to global bifurcations, which are, in general, mediated by the stable and unstable manifolds of certain periodic orbits of saddle type. Examples for such global bifurcations are homoclinic bifurcations^{16–18} and different types of crises.¹⁹ Both phenomena have been studied theoretically and observed in several experiments with physical systems.^{20,21} Homoclinic bifurcations are connected to the formation of a homoclinic orbit (or separatrix loop) associated with a saddle equilibrium state. Depending on the eigenvalues of the equilibrium state one distinguishes saddle-node-, saddle-focus- or bifocus-type scenarios.¹⁶ One of the characteristic features of a homoclinic bifurcation is the exponential growth of the times needed to return to a Poincaré surface of section for orbits in the neighborhood of the homoclinic orbit. Thus, the divergence of the return time can be used as an indicator for the appearance of a homoclinic bifurcation.

Usually, the only observable which is accessible in electrophysiological experiments is the interspike intervals re-

corded from a spike train of action potentials. These interspike intervals can be regarded as direct measurements of the Poincaré return time.^{22,23} From this point of view measurement techniques usually used in the study of neurobiological systems are very convenient to investigate homoclinic bifurcations.

The dynamics of biological neurons is always contaminated with high-dimensional random processes, or “noise.” For subthreshold regimes noise might play a constructive role leading to more coherent behavior of neuron systems via mechanisms of stochastic²⁴ or coherent²⁵ resonances. However, noise usually destroys the fine bifurcation structure of a dynamical system, and, therefore, turns the bifurcation analysis into a hard statistical problem. Here we address these difficulties by studying the behavior of a modified Hodgkin–Huxley (MHH) model,¹ with and without added noise, comparing the results with those observed in electrophysiological experiments.

The topological structure of the chaotic attractor of this system has been studied in Ref. 26, while several specific dynamical properties of this model, for example, the period doubling cascade to chaos and specific resonance phenomena, have been studied in Ref. 27. In this paper we focus on global bifurcation phenomena in the MHH model. In particular we provide numerical evidence for the occurrence of a homoclinic bifurcation in the modified Hodgkin–Huxley model, show its robustness to noise, and also demonstrate similar dynamic behavior in electrophysiological experiments with the crayfish caudal photoreceptor.

II. THE MODEL

The MHH model of thermally sensitive neurons has been proposed by Braun *et al.*¹ and mimics all spike train patterns observed in electroreceptors from dogfish,⁴ and catfish,¹¹ and from facial cold receptors¹¹ and hypothalamic neurons of the rat.²⁸ All these neurons can be characterized by spontaneous, noisy oscillations which are reflected in the spike trains. The classical HH model,²⁹ on the one hand, has been simplified (e.g., no inactivation terms), but on the other hand, has been extended by two additional slow currents according to the experimental findings of spike-independent oscillations (see above). The stochastic term produces more realistically looking simulations, e.g., makes the transitions between different impulse patterns more smooth, and is necessary to account for subthreshold oscillations with skipings when high-temperature ranges are considered (which, however, are not in the scope of this paper). The MHH model has been described in detail in Ref. 1, and so will not be elaborated here. It is given by the usual equation for the membrane potential,

$$C_M \frac{dV}{dt} = -I_l - I_d - I_r - I_{sd} - I_{sr} + \xi(t), \quad (1)$$

where C_M is the membrane capacitance, V is the membrane potential, and I_l is the leakage current, which can be written as $I_l = g_l(V - V_l)$. I_d and I_r are simplified fast Hodgkin–Huxley currents representing Na and K channels, respectively, which account for spike generation, I_{sd} and I_{sr} are the

slow currents which account for the oscillations, and $\xi(t)$ is the noise. The voltage-dependent currents I_d , I_r and I_{sd} are

$$I_k = \rho(T)g_k a_k(V - V_k), \quad (2)$$

where the index k stands for d , r or sd currents, $\rho(T)$ is the temperature-dependent scaling factor for the ionic currents, g_k is the maximum conductance and V_k is the reversal potential. The activation variable is a_k and is described by the differential equation

$$\frac{da_k}{dt} = \frac{\phi(a_{k\infty} - a_k)}{\tau_k}. \quad (3)$$

This equation serves I_r and I_{sd} currents. I_{sd} is considered to be a mixed current which mainly is carried by sodium ions and to a minor part by calcium ions which, however, are essential for activation of I_{sr} . I_{sr} represents a calcium-dependent potassium current where the dynamics of internal changes are given by the equations for the activation variable a_{sr} . In Eq. (3) $\phi = \phi(T)$ is the temperature-dependent scaling factor for activation, τ_k is the time constant and $a_{k\infty}$ is the steady-state activation:

$$a_{k\infty} = [1 + \exp(-s_k(V - V_{0k}))]^{-1} \quad (4)$$

with s_k the steepness and V_{0k} the half-activation value. For the sodium current, I_d , we adopt $I_d = \rho g_d a_{d\infty}(V - V_d)$, as the sodium current changes much faster than other ionic currents. For the current I_{sr} the activation variable a_{sr} is governed by

$$\frac{da_{sr}}{dt} = \frac{\phi(-\eta I_{sd} - \theta a_{sr})}{\tau_{sr}}, \quad (5)$$

where the constant η serves for increasing $[Ca^{2+}]$ following I_{sr} , while θ accounts for active elimination of intracellular calcium. The temperature-dependent factors are defined as

$$\rho = A_1^{(T-T_0)/10}, \quad \phi = A_2^{(T-T_0)/10}, \quad (6)$$

where $A_1 = 1.3$, $A_2 = 3$ and $T_0 = 25^\circ C$.

Thus the model is represented by four differential equations: the first is for the membrane potential V , the second is for the activation of the potassium current a_r , the third is for the activation of the subthreshold depolarization current a_{sd} , and the fourth is for the activation of the subthreshold repolarization current a_{sr} . In numerical simulations the parameter values are $g_{sd} = 0.25 \text{ mS/cm}^2$, $g_{sr} = 0.4 \text{ mS/cm}^2$, $g_d = 1.5 \text{ mS/cm}^2$, $g_r = 2.0 \text{ mS/cm}^2$, $g_l = 0.1 \text{ mS/cm}^2$, $\tau_{sd} = 10 \text{ ms}$, $\tau_{sr} = 20 \text{ ms}$, $\tau_r = 2.0 \text{ ms}$, $s_d = -0.25 \text{ mV}^{-1}$, $s_r = -0.25 \text{ mV}^{-1}$, $s_{sd} = 0.09 \text{ mV}^{-1}$, $V_{0d} = -25 \text{ mV}$, $V_{0r} = -25 \text{ mV}$, $V_{0sd} = -40 \text{ mV}$, $\eta = 0.012$, $\theta = 0.17$, $V_{sd} = V_d = 50 \text{ mV}$, $V_{sr} = V_r = -90 \text{ mV}$, $V_l = 60 \text{ mV}$, and $C_M = 1 \text{ }\mu\text{F/cm}^2$. These parameter values yield a good agreement of the model with the experimentally observed temperature dependence of spike train patterns. For more details of the model and comparison with experiment, see Ref. 1.

III. BIFURCATIONS IN THE MODIFIED HODGKIN-HUXLEY NEURON MODEL

The MHH model has been simulated numerically first in the absence of noise. For an easy comparison with electro-

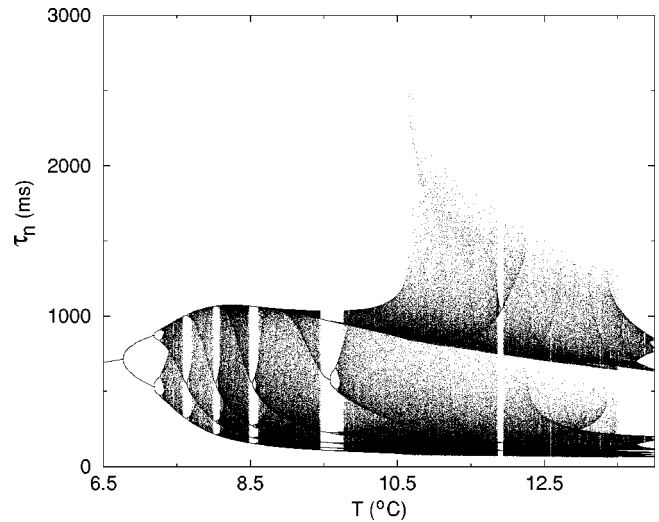


FIG. 1. Bifurcation diagram of the MHH system. The deterministic case.

physiological experiments, we use the interspike intervals, τ_n , as a state variable. The interspike intervals are registered by the membrane potential crossing a threshold (at -20 mV) with positive derivative (Poincaré surface of section). Note that for oscillatory neuron models they can be associated with the instantaneous period of the action potential, while τ_{n+1} versus τ_n represents the first return map of the system.

The bifurcation diagram of the MHH is shown in Fig. 1 and represents a classical route to chaos through a period-doubling cascade³⁰ up to a temperature $T \approx 10^\circ C$. The first period doubling bifurcation occurs at $T_1 \approx 6.765^\circ C$, the second at $T_2 \approx 7.195^\circ C$. Finally, for $T > T_{ch} \approx 7.31^\circ C$ the system becomes chaotic. Inside the chaotic region we observe several periodic windows opened by a saddle-node bifurcation and closed by a global bifurcation, namely an interior crisis. This picture is very similar to that of the logistic map, for example, the return map $\tau_{n+1} = f(\tau_n)$ looks like a logistic map for $T < 8.5^\circ C$, that is, a parabola with a single maximum. However, with further increase of the temperature the shape of the return map changes from parabolic to a curve with multiple maxima.

The focus of our interest is the abrupt increase of the duration of the interspike intervals in the region $10.658^\circ C < T < 10.9^\circ C$ (see Fig. 1). For $T < T_{cr} = 10.6589^\circ C$ the duration of the interspike intervals is not larger than 1600 ms. At $T = T_{cr}$ an abrupt explosion of the interspike intervals occurs. In Fig. 2 we show the return map before and after this transition. We see that after the transition an additional, well-separated part of the return map with longer time intervals appears. This transition is well pronounced in the return map, but it is difficult to recognize in the phase space of the system: before and after the transition the phase portraits of the system have nearly the same structure. Thus, the signature of this transition in phase space is the appearance of a new type of orbits within the attractor.

Let us study the explosion in the interspike intervals in detail. As mentioned above, long time intervals between consecutive returns to a Poincaré section can be considered as an indicator for the approach of a homoclinic orbit. Such a ho-

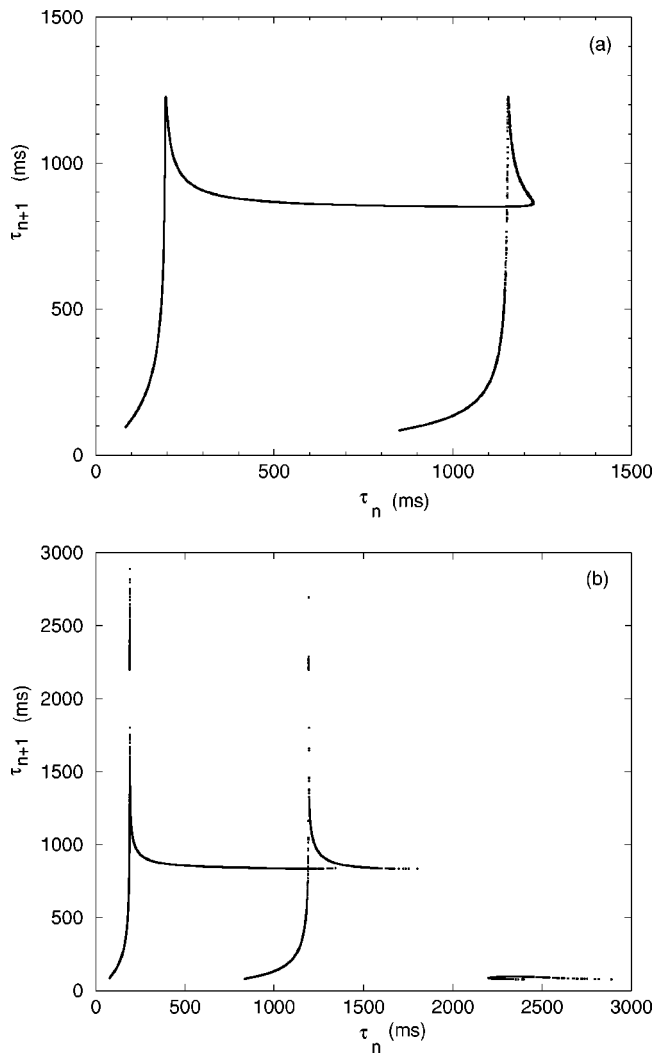


FIG. 2. The return map $\tau_{n+1}=f(\tau_n)$ for two parameters values: (a) $T=10.6^\circ\text{C}$ and (b) $T=10.7^\circ\text{C}$.

moenic orbit is associated with an equilibrium state of saddle type and its stable and unstable manifolds. In our case this saddle equilibrium is embedded in the already existing chaotic attractor. It has two stable and two unstable directions. The eigenvalues, corresponding to the stable directions, are real ($\lambda_1 < 0, \lambda_2 < 0$) while the eigenvalues, corresponding to the unstable directions, are complex ($\gamma_{1,2} = \rho \pm i\omega, \rho > 0$). Thus we have an equilibrium state of saddle-focus type. If we suppose that there exists a chaotic set with an embedded homoclinic orbit, then the eigenvalues of the equilibrium state should satisfy the Shilnikov condition:¹⁸ $-\lambda > \rho$. Indeed, the eigenvalues at a temperature value $T = 10.7456^\circ\text{C}$, which is, as we will show, close to the homoclinic bifurcation, are: $\lambda_1 = -0.182$, $\lambda_2 = -0.146$, $\gamma_{1,2} = 0.327 \times 10^{-2} \pm i0.282 \times 10^{-2}$ [the units of the eigenvalues are in $(\text{ms})^{-1}$]. From those values one can see that the two real eigenvalues are comparable in magnitude. For this reason one cannot easily reduce the problem to the known cases of homoclinic bifurcations in R^3 .

In this model we have to deal with an equilibrium state of saddle-focus type having a two-dimensional stable and a two-dimensional unstable manifold. The return time for the

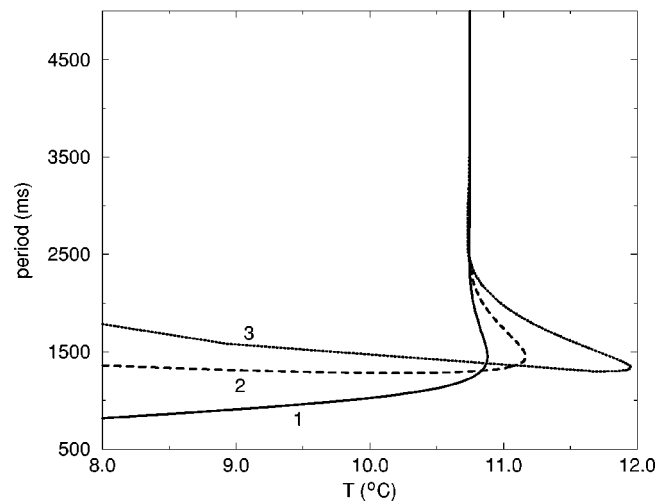


FIG. 3. Periods of different limit cycles versus temperature: (1, solid line) the period-1 cycle, (2, dashed line) the period-2 cycle, and (3, dotted line) the period-3 cycle.

homoclinic orbit itself is infinity. A separatrix loop is built up, where the outgoing path is tangent to the unstable manifold while the returning path is tangent to the stable manifold of the equilibrium state. Nearby trajectories on the attractor approach the equilibrium state along its stable manifold. The motion slows down so that the trajectory spends a long time in the neighborhood of the equilibrium state before it is ejected along the unstable manifold. The same happens to saddle limit cycles embedded in the attractor. If they are close to the homoclinic orbit, then at least one point of the saddle limit cycle is close to the saddle equilibrium state. As a consequence the Poincaré return time of these saddle limit cycles, that is their period, becomes also very large. The motion on the saddle limit cycle slows down approaching the vicinity of the equilibrium state along its stable manifold. In Fig. 3 we show the dependencies of the periods of different limit cycles versus the control parameter calculated using the continuation software CONTENT.³¹ In particular, we show the period-1 cycle (which is born from the equilibrium point in a Hopf bifurcation), the period-2 cycle (which is born from the period-1 cycle through a period-doubling bifurcation at $T \approx 6.765^\circ\text{C}$), and the period-3 cycle [which is born via saddle-node bifurcation at $T \approx 7.58^\circ\text{C}$ (see Fig. 1)]. Although these cycles possess turning points at different temperature values, their periods diverge at the same temperature value $T \approx 10.7456^\circ\text{C}$. Extensive calculations have shown qualitatively the same behavior for other limit cycles of higher periods: they are accumulated and their periods diverge at $T \approx 10.7456^\circ\text{C}$.

The computation of the homoclinic orbit itself using direct numerical methods or perturbation methods is rather difficult since the saddle-focus has a two-dimensional stable and two-dimensional unstable manifold with two stable real eigenvalues very close to each other. Therefore, we can show the evidence of the homoclinic bifurcation only by the discussed indirect indicators.

The phase portrait of the system reflects the behavior discussed above. In Fig. 4 we show a two-dimensional pro-

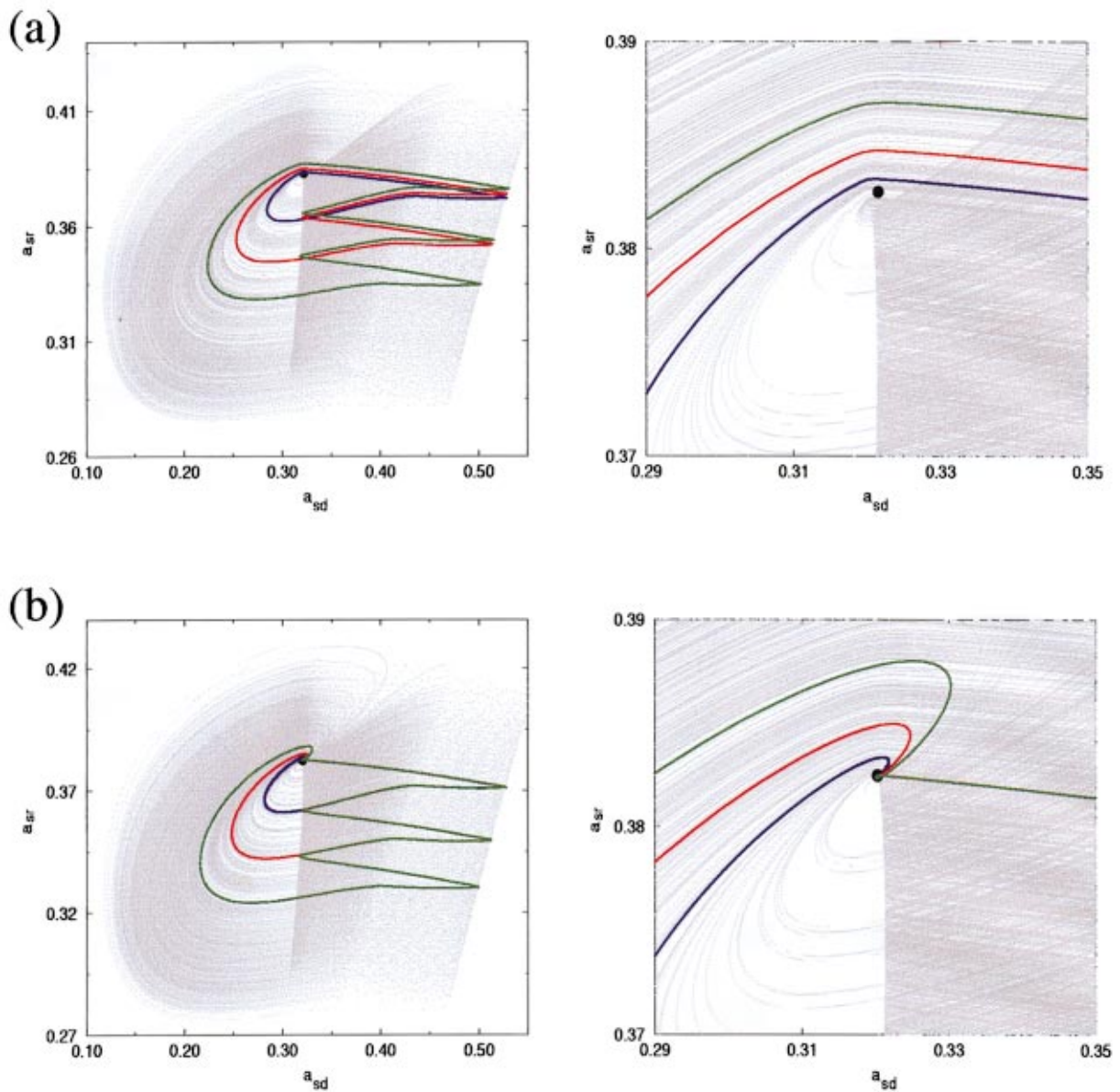


FIG. 4. (Color) Two-dimensional projection of the phase portrait of the system at $T=10.65\text{ }^{\circ}\text{C}$ (a) and $T=10.7456\text{ }^{\circ}\text{C}$ (b). A neighborhood of the saddle-focus equilibrium point is also shown. The gray dots represent the chaotic attractor; the black-filled circle is the saddle-focus equilibrium state; the unstable limit cycles of periods 1, 2 and 3 are shown by blue, red, and green bold lines, respectively.

jection of the chaotic attractor for two parameter values: one before the suspected homoclinic bifurcation and the other at the temperature value where we find the divergent behavior discussed above. We also plot the saddle cycles and the saddle-focus equilibrium point. At $T=10.65\text{ }^{\circ}\text{C}$, that is before the suspected bifurcation, the saddle-focus is not included into the saddle cycles. The saddle cycles are located far from each other. However, at the temperature $T=10.7456\text{ }^{\circ}\text{C}$ the saddle cycles are extremely close to the saddle-focus. Moreover, they are extremely close to each other, that is, the period-1 cycle is a part of the period-2 cycle, the period-2 cycle is a part of the period-3 cycle and so on. At the same time, as it can be seen from the figure, a large fraction of the phase trajectories passes the vicinity of the saddle focus. Unfortunately, we were not able to compute the homoclinic orbit itself, but each of the presented saddle

orbits can be considered as a candidate for it.

We note that, as soon as the phase trajectory approaches the vicinity of the equilibrium state, the motion of the system slows down, so that the phase trajectory spends a long time in the neighborhood of the equilibrium state. This gives rise to very long interspike intervals. To support this argument we present in Fig. 5 the dependence of the minimal distance between the saddle-focus and the trajectory on the chaotic attractor versus control parameter and the maximal residence time of the phase trajectory spent in a small neighborhood of the equilibrium state. As can be seen, the distance becomes very small at a certain parameter value and the phase trajectories of the system spend a maximal time near the equilibrium state. These plots together with the discussed bifurcation diagram suggest that the homoclinic bifurcation occurs at $T\approx 10.7456\text{ }^{\circ}\text{C}$.

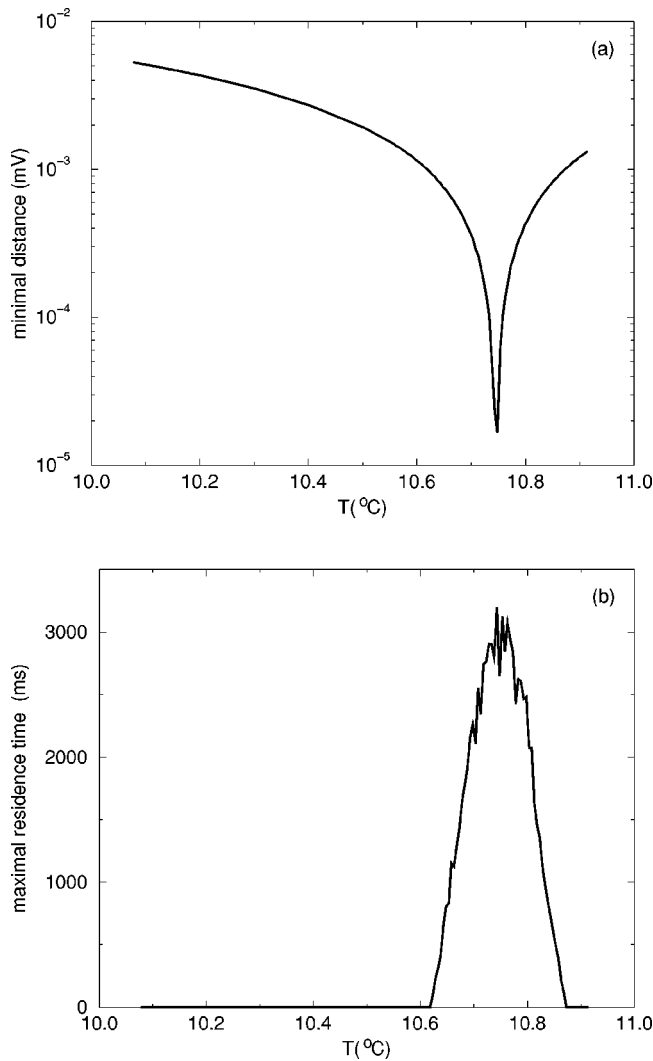


FIG. 5. (a) Minimal distance between the saddle-focus equilibrium state and the trajectories on the chaotic attractor versus control parameter. (b) Maximal residence time of the trajectories in a small neighborhood ($\delta=0.01$) of the saddle-focus.

IV. STATISTICAL PROPERTIES OF THE RETURN MAP

Our numerical simulations have shown that in the vicinity of the transition to the existence of very long interspike intervals [see, e.g., Fig. 2 (b)] the system spends a long time in the first region of relatively short interspike intervals ($\tau_n < 1600$) and very seldomly visits the second region with rather long intervals. This process, therefore, displays an intermittency between the region of the return map with short interspike intervals and the second region represented by long intervals. Within the second region of long intervals the trajectory on the attractor comes very close to the saddle-focus associated with the homoclinic orbit yielding long return times. Intermittent processes in chaotic systems are usually characterized by a power law scaling of the mean time interval between bursts, $\langle \tau \rangle$, with overcriticality $|T - T_{cr}|$.³⁰ In our case $\langle \tau \rangle$ is represented by the mean length of trajectory segments of short interspike intervals in-between two bursts, i.e., two events with long interspike intervals. The numerically found critical parameter value $T_{cr}=10.659^\circ\text{C}$ denotes the onset of intermittency. In order to verify whether

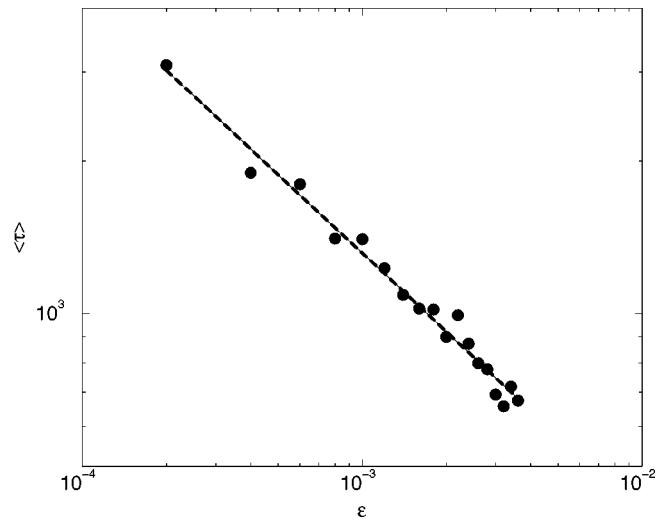


FIG. 6. Mean length between bursts $\langle \tau \rangle$ versus overcriticality $\epsilon = T - T_{cr}$ (circles) and power law fit (dashed line) $\epsilon^{-\gamma}$, $\gamma \approx 0.52$.

this type of behavior can also be found for intermittent behavior close to a homoclinic bifurcation we calculated $\langle \tau \rangle$ as a function of $|T - T_{cr}|$ for 2×10^5 interspike intervals for each parameter value. The result is shown in Fig. 6 and is fairly well described by the power law $\langle \tau \rangle \propto (T - T_{cr})^{-\gamma}$ with the slope $\gamma \approx 0.52$. Thus, we obtain a similar exponent γ as for other intermittent processes in chaotic systems.

V. NOISE INFLUENCE ON THE MHH MODEL

Since all biological systems are inherently noisy, it is necessary to test how robust the above described transition is against noise. For this purpose we include an additive white Gaussian noise $\xi(t)$, $\langle \xi(t) \rangle = 0$, $\langle \xi(t) \xi(t+s) \rangle = 2D \delta(s)$, where D is the intensity, into the first equation of the MHH for the membrane potential and study numerically the corresponding set of stochastic differential equations. It turns out that the system is extremely sensitive to this noise. The bifurcation diagram of the noisy system is shown in Fig. 7 for

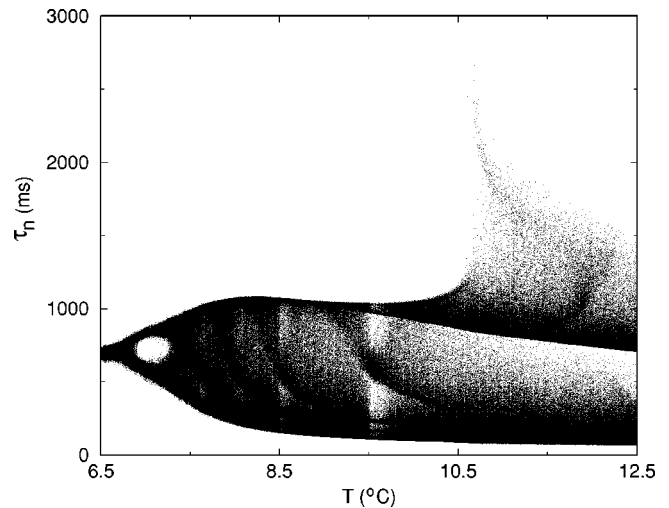


FIG. 7. Bifurcation diagram of the stochastic MHH system with $D = 0.001$.

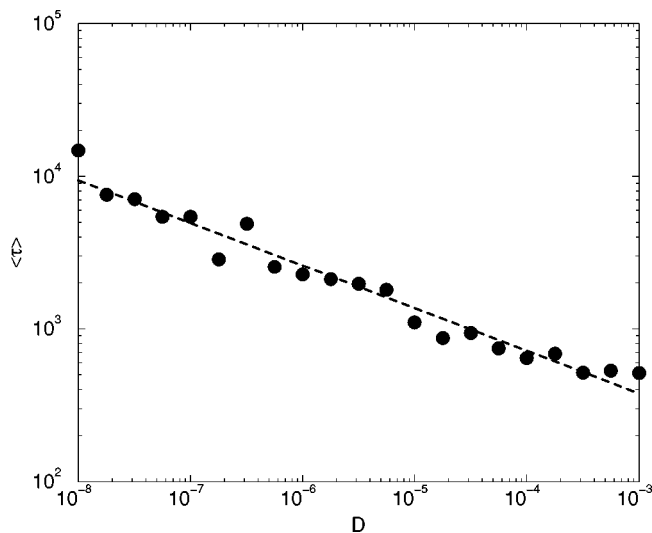


FIG. 8. Mean length between bursts $\langle \tau \rangle$ versus noise intensity D (circles) and power law fit (dashed line) $D^{-\alpha}$, $\alpha=0.27$ at the critical point $T = T_{cr}$.

$D=0.001$. Although almost all fine structure of the bifurcation diagram is blurred by the noise, the transition studied above in a noiseless system is still well pronounced: again at a certain value of the temperature there is an explosion of interspike intervals. However, the transition appears to be smoothed and the critical parameter values are shifted towards smaller values of temperature.

Let us discuss the statistical properties of intermittency near the explosion of interspike intervals. To reveal the scaling of the noise-driven system we follow recipes of Ref. 32, where the noise influence on crisis-induced intermittency has been studied. According to the theoretical prediction of the above-mentioned study, the mean time between bursts versus noise intensity, calculated at the onset of intermittency of the noise-free system, scales with noise intensity D by the power law $\langle \tau \rangle \propto D^{\gamma/2}$, where γ is scaling exponent of the noise-free system.

We calculate the mean length of trajectory segments with only short interspike intervals between two events with long interspike intervals versus noise intensity at the critical point $T=T_{cr}$. The dependence of $\langle \tau \rangle(T_{cr})$ versus noise intensity is shown in Fig. 8 and is well scaled by the power law $D^{-\alpha}$ with the scaling constant $\alpha \approx 0.27$. The good agreement with the expected value $\gamma/2=0.26$ is a strong indication that a similar scaling relation as for the crisis-induced intermittency holds also for the noise perturbed homoclinic bifurcation.

VI. PHYSIOLOGICAL EVIDENCE OF THE HOMOCLINIC BIFURCATION

As stated above, only indirect evidence of the homoclinic bifurcation can be expected from actual physiological experiments. In particular, we seek evidence of an explosion of the interspike time intervals using temperature as the control parameter. Moreover, one must search in sensory neurons which are known to exhibit subthreshold oscillators similar to those described by the MHH model. In this sec-

tion, we offer qualitative evidence of the homoclinic bifurcation obtained from extracellular recordings of the discharges from the caudal photoreceptor cell embedded in the crayfish sixth, or terminal, ganglion. Indeed period-1 unstable periodic orbits¹³ and other noisy periodic behavior³³ have previously been observed in this system.

The preparation has been described previously³³ but will be very briefly reviewed here. Crayfish (*Procambarus clarkii*) of approximately 1 year of age were obtained. The abdomen and tailfan were isolated quickly and fixed ventral side up in a dissection chamber filled with crayfish saline solution. The exoskeleton and muscles were removed in order to expose the sixth or terminal ganglion. The intact caudal photoreceptor (CPR) cell was then removed from the sixth ganglion and transferred to a recording chamber where the temperature of the saline bath was controlled. An extracellular electrode was attached to the CPR cell, and long sequences of action potentials (spike trains) were recorded at various bath temperatures.

Our data are presented as the record of interspike time intervals versus temperature as shown by the three panels in Fig. 9. These records were obtained from three separate animals. All three show at least qualitative evidence of the homoclinic bifurcation in the form of an explosion of the interspike time intervals that occurs at a more-or-less identifiable critical temperature. The best indication is shown in Fig. 9(a), where the onset of the explosion occurs with decreasing temperature at approximately 8.3 °C. This recording is particularly interesting, because it clearly shows the initial period doubling bifurcation at about 13.5 °C followed by what appears to be a chaotic region. Moreover, this region includes at least two periodic windows at $T \approx 10.8$ °C and 12.1 °C. Similar evidence of a period doubling bifurcation followed by an explosion of interspike intervals at low temperatures has been obtained for the rat cold receptor neuron, as shown in Fig. 6 of Ref. 15. The recordings shown in Figs. 9(b) and 9(c) are less clear, but both show the explosion upon increasing temperature. Figure 9(b) also shows some evidence of the period doubling bifurcation at $T \approx 9.2$ °C.

Not all CPR cells show this behavior. We tested 16 CPR cells from 16 different animals. Of these only four showed evidence of the bifurcation. Moreover, we emphasize that the physiological evidence presented here is only qualitative. Nevertheless, it is indicative and suggests further experiments as well as an explanation for time interval explosions observed in pacemaker cells grounded in the nonlinear dynamics of the underlying chaotic attractor.

VII. SUMMARY

We have analyzed the bifurcation structure of a modified Hodgkin–Huxley-type model to explain an explosion of interspike intervals in terms of a homoclinic bifurcation. There are a number of arguments which support this explanation, namely the exponential growth of the Poincaré return times of saddle periodic orbits with different periods and their closeness to the saddle equilibrium state embedded in the attractor. We obtained an accumulation of these saddle periodic orbits as we approach the homoclinic bifurcation. Close

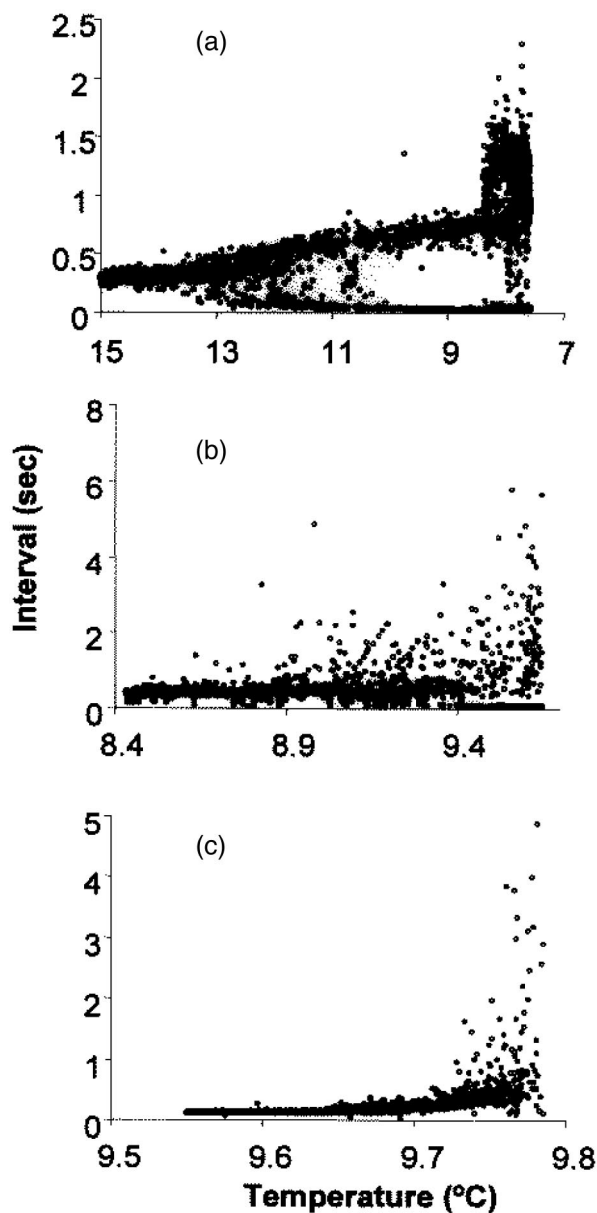


FIG. 9. Interspike time interval recordings versus temperature of the saline bath for three different crayfish caudal photoreceptor cells.

to the expected homoclinic orbit we find an intermittency between stretches of trajectories with only short interspike intervals and excursions to long interspike intervals. The described bifurcation picture suggests the following mechanism for the observed explosion of the interspike intervals. As we approach the homoclinic bifurcation of the saddle equilibrium state, the phase trajectory on the chaotic attractor spends a considerable amount of time in the vicinity of the saddle-focus equilibrium point. This leads to the appearance of very long interspike intervals. At the onset of this transition the phase trajectories reach the neighborhood of the saddle-focus very rarely, so that the long interspike intervals appear very seldom too. With the increase in the control parameter, the system approaches the homoclinic bifurcation; the phase trajectories come closer and more frequently to the saddle-focus. As a result a larger number of the long interspike intervals appears and the mean length between

bursts decreases. The divergent behavior of interspike intervals can be observed for both cases of increasing and decreasing temperature, when the control parameter approaches the homoclinic bifurcation.

It is important to note that averaged characteristics usually calculated in electrophysiology, e.g., mean firing rate, are insensitive to the complex behavior discussed in this paper. The existence of a global bifurcation and its drastical consequence, that is, the explosion of the interspike intervals, suggests that the temporal code might be an appropriate encoding scheme for thermoreceptors. Specifically, the occurrence of long interspike intervals probably indicates the approach to painful temperatures, while the explosion of interspike intervals, which, as we have shown, occurs due to the homoclinic bifurcation, physiologically means a blockage of neuron activity. Furthermore, this transition is robust against noise and is observable in the experiment. However, further experiments are necessary to understand the physiological significance of the phenomenon studied here.

ACKNOWLEDGMENTS

We are grateful to B. Eckhardt who originally suggested this study. We thank M. Zaks, L. P. Shil'nikov, A. L. Shil'nikov and P. Glendinning for stimulating discussions and essential insights. This work was supported by the U. S. Office of Naval Research, The Fetzer Institute, the Department of Energy and the German Research Foundation (DFG).

- ¹H. A. Braun, M. T. Huber, M. Dewald, K. Schäfer, and K. Voigt, *Int. J. Bifurcation Chaos Appl. Sci. Eng.* **8**, 881 (1998).
- ²H. Hensel, K. H. Andres, and M. von Düring, *Pflugers Arch. Ges. Physiol. Menschen Tiere* **352**, 1 (1974).
- ³H. A. Braun, H. Bade, and H. Hensel, *Pflugers Arch. Ges. Physiol. Menschen Tiere* **386**, 1 (1980).
- ⁴H. A. Braun, H. Wissing, K. Schäfer, and M. C. Hirsch, *Nature (London)* **367**, 270 (1994).
- ⁵K. Schäfer, H. A. Braun, and L. Rempe, *Experientia* **47**, 47 (1991).
- ⁶K. Schäfer, H. A. Braun, and C. Isenberg, *J. Gen. Physiol.* **88**, 557 (1986).
- ⁷T. Toth and V. Crunelli, *NeuroReport* **3**, 65 (1992).
- ⁸X. J. Wang, *NeuroReport* **5**, 221 (1993).
- ⁹T. R. Chay, Y. S. Fan, and Y. S. Lee, *Int. J. Bifurcation Chaos Appl. Sci. Eng.* **5**, 595 (1995).
- ¹⁰A. Longtin and K. Hinzer, *Neural Comput.* **8**, 215 (1995).
- ¹¹H. A. Braun, K. Schäfer, K. Voigt, R. Peters, F. Bretschneider, X. Pei, L. Wilkens, and F. Moss, *J. Comp. Neurosci.* **4**, 335 (1997).
- ¹²M. Huber, J. Kriegel, M. Dewald, K. Voigt, and H. A. Braun, *Biosystems* **48**, 95 (1998).
- ¹³X. Pei and F. Moss, *Nature (London)* **379**, 618 (1996).
- ¹⁴H. A. Braun, K. Schäfer, K. Voigt, R. Peters, F. Bretschneider, X. Pei, L. Wilkens, and F. Moss, *J. Comp. Neurosci.* **4**, 335 (1997).
- ¹⁵H. A. Braun, M. Dewald, K. Voigt, M. Huber, X. Pei, and F. Moss, *Neurocomputing* **26**, 79 (1999).
- ¹⁶L. P. Shil'nikov, *Math. USSR Sb.* **10**, 91 (1970).
- ¹⁷C. Tresser, *Ann. Inst. H. Poincaré Physique Théorique* **40**, 441 (1984).
- ¹⁸P. Glendinning, in *New Directions in Dynamical Systems*, edited by T. Bedford and J. Swift (Cambridge U. P., Cambridge, 1987).
- ¹⁹C. Grebogi, E. Ott, and J. A. Yorke, *Phys. Rev. Lett.* **48**, 1507 (1982); *Physica D* **7**, 181 (1983).
- ²⁰R. W. Rollins and E. R. Hunt, *Phys. Rev. A* **29**, 3327 (1984).
- ²¹J. C. Sommerer, W. L. Ditto, C. Grebogi, E. Ott, and M. L. Spano, *Phys. Rev. Lett.* **66**, 1947 (1991).
- ²²T. Sauer, *Phys. Rev. Lett.* **72**, 3811 (1994); *Chaos* **5**, 127 (1995).
- ²³N. B. Janson, A. N. Pavlov, A. B. Neiman, and V. S. Anishchenko, *Phys. Rev. E* **58**, R4 (1998).

- ²⁴K. Wiesenfeld and F. Moss, *Nature (London)* **373**, 33 (1995).
- ²⁵A. Pikovsky and J. Kurths, *Phys. Rev. Lett.* **78**, 775 (1997).
- ²⁶R. Gilmore, X. Pei, and F. Moss, *Chaos* **9**, 812 (1999).
- ²⁷W. Braun, B. Eckhard, H. A. Braun, and M. Huber, *Phase Space Structure of a Thermoreceptor* (submitted to *Phys. Rev. E*).
- ²⁸M. Dewald, H. A. Braun, K. Voigt, X. Pei, and F. Moss (unpublished).
- ²⁹See, for example, B. Hille, *Ionic Channels of Excitable Membranes*, 2nd ed. (Sinauer, Sunderland, MA, 1992), Chap. 2.
- ³⁰E. Ott, *Chaos in Dynamical Systems* (Cambridge U. P., Cambridge, 1993).
- ³¹Y. Kuznetsov, *Elements of Applied Bifurcation Theory* (Springer-Verlag, New York, 1995); *CONTENT - integrated environment for analysis of dynamical system* (available at: ftp.cwi.nl).
- ³²J. C. Sommerer, E. Ott, and C. Grebogi, *Phys. Rev. A* **43**, 1754 (1991).
- ³³X. Pei, L. Wilkens, and F. Moss, *J. Neurophysiol.* **76**, 3002 (1996).